Constraints on the non-linear coupling parameter f_{nl} using the CMB

A. Curto, E. Martínez-González, R. B. Barreiro

Abstract We present a review of the constraints on the non-linear coupling parameter f_{nl} using the Cosmic Microwave Background (CMB) temperature anisotropies at high resolution. In particular we summarise the recent results presented in the analysis by [9] and compare it with other works.

In [9] several third order estimators based on the spherical Mexican hat wavelet are considered. These quantities are combined to perform a χ^2 analysis. The χ^2 statistic is used to test the Gaussianity of the data as well as to constrain the f_{nl} parameter using the WMAP data. This analysis is based on simulations that take into account the CMB and the instrumental properties.

Most of the analyses confirm that the data of these experiments are compatible with Gaussianity. The best estimate at present of the non-linear coupling parameter is $-8 < f_{nl} < +111$ at 95 per cent CL [9] using wavelets.

1 Introduction

The temperature fluctuations of the CMB can be used to put tight constraints on the cosmological parameters. The Big Bang theory and inflation are our best theories to describe the universe. In particular, the standard, single field, slow roll inflation

A. Curto
Instituto de Física de Cantabria, CSIC-Universidad de Cantabria and Dpto. de Física Moderna, Universidad de Cantabria, Avda. de los Castros s/n, 39005 Santander, Spain, e-mail: curto@ifca.unican.es

E. Martínez-González
Instituto de Física de Cantabria, CSIC-Universidad de Cantabria, Avda. de los Castros s/n, 39005 Santander, Spain.

R. B. Barreiro
Instituto de Física de Cantabria, CSIC-Universidad de Cantabria, Avda. de los Castros s/n, 39005 Santander, Spain.

[14] predicts that the primordial density fluctuations are compatible with a nearly Gaussian random field. However, different primordial processes (as for example topological defects) can introduce non-Gaussian features at certain levels that may be detectable [6]. Also, several non-standard models of inflation predict a detectable level of non-Gaussianity in the primordial gravitational potential (see, e.g. [1] and references therein).

The search of non-Gaussian deviations in the CMB has become a question of considerable interest, as it can be used to discriminate different possible scenarios of the early universe and also to study the secondary sources of non-Gaussianity.

High precision CMB experiments are sensitive to deviations due to second-order effects in perturbation theory, usually parametrised through the local non-linear coupling parameter f_{nl}. This kind of non-Gaussianity is produced following a model which introduces a quadratic term in the primordial gravitational potential [24, 12, 16]

$$\Phi(\mathbf{x}) = \Phi_L(\mathbf{x}) + f_{nl}\{\Phi_L^2(\mathbf{x}) - \langle\Phi_L^2(\mathbf{x})\rangle\} \quad (1)$$

where $\Phi(\mathbf{x})$ is a linear random field which is Gaussian distributed and has zero mean.

This work is a summary of the analyses presented in [9] and other articles (see Table 1) using the data collected by WMAP and other experiments. The analysis is based on the Spherical Mexican Hat Wavelet (SMHW) as defined in [23]. In Section 2 we describe the wavelet and the third order estimators. The results of the Gaussianity analysis and the constraints on f_{nl} using wavelets are revisited in Section 3. In Section 4 we present a list of results on the limits on f_{nl}. Finally our conclusions are summarised in Section 5.

2 Methodology

Several methods can be used to test the Gaussianity of the CMB and to constrain f_{nl}. We can mention the SMHW, (used recently in [9]), the Minkowski functionals (see for example [15]) and the angular bispectrum (see for example [20]).

2.1 The SMHW and the estimators

The spherical wavelets have been applied in some analyses to test the Gaussianity of different data sets (see [9] for a list of examples). Given a function $f(\mathbf{n})$ evaluated on the sphere at a direction $\mathbf{n}$ and the SMHW family on that space, $\Psi(\mathbf{n};\mathbf{b},R)$, we define the continuous wavelet transform as

$$w(\mathbf{b};R) = \int d\mathbf{n} f(\mathbf{n})\Psi(\mathbf{n};\mathbf{b},R) \quad (2)$$

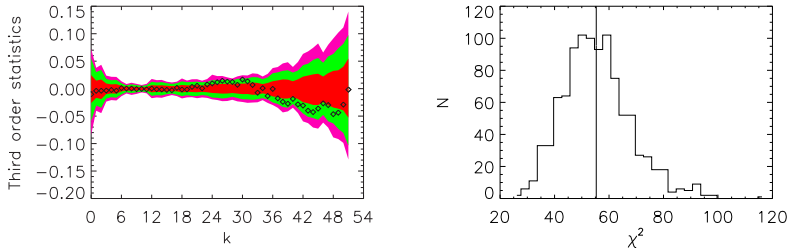

Fig. 1 Left panel: the third order statistics corresponding to the V+W WMAP data (diamonds). We also plot the acceptance intervals for the 68% (inner in red), 95% (middle in green), and 99% (outer in magenta) significance levels given by 1000 V+W Gaussian simulations of signal and noise. Right panel: the χ^2 distribution of 1000 V+W Gaussian simulations of signal and noise. The vertical line corresponds to the value obtained from the data.

where **b** is the position on the sky at which the wavelet coefficient is evaluated and R is the scale of the wavelet.

The estimators used in [9] are third order combinations of the wavelet coefficients (Eq. 2) evaluated at several scales from 6.9 arc minutes to 150 arc minutes (see [9] for a detailed description of the considered scales). These estimators are combined to perform a χ^2 test by comparing the WMAP data with the expected values of the Gaussian model and non-Gaussian model with f_{nl} (see Eqs. 7 and 8 of [9]).

3 Results

3.1 Gaussianity analysis with the SMHW

The data analysed in [9] are the 5-year WMAP foreground reduced data maps at the frequency bands of 41 GHz (Q band), 61 GHz (V band) and 94 GHz (W band). The maps per different radiometers are combined using the inverse of the noise variance as an optimal weight. In particular the Q+V+W, Q, V, W, and V+W maps are considered. The third order estimators are computed for the WMAP data and for a set of 1000 Gaussian simulations. As we can see in the left panel of Fig. 1 the V+W data are compatible with Gaussian simulations. The results of a χ^2 test for the V+W data are in the right panel of Fig. 1. The vertical line corresponds to the χ^2 of the V+W data and the histogram corresponds to the χ^2 of 1000 Gaussian simulations. Similar results are obtained for the Q, V, W, and Q+V+W combined maps.

3.2 Constraints on f_{nl} with the SMHW

The constraints on f_{nl} presented in [9] are computed using the considered WMAP data maps and realistic non-Gaussian simulations (see [21, 22] for a description of these simulations). They also consider Gaussian simulations in order to obtain the frequentist error bars.

In Fig. 2 we present a plot of $\chi^2(f_{nl})$ versus f_{nl} for the combined V+W WMAP data and a histogram of the best fit f_{nl} for 1000 Gaussian simulations of the combined V+W map. After considering the contribution of point sources (using a model based on the work by [11]) the best estimate of f_{nl} is $-8 < f_{nl} < +111$ at 95%CL.

4 Constraints on f_{nl} from other analyses

Several methods have been used to constrain f_{nl} using the data from different CMB experiments. The first observational limit on f_{nl} was established by [17] from the COBE data using the angular bispectrum. The wavelets were used to test Gaussianity and constrain this parameter in [3]. Recent experiments as WMAP and some balloon-borne experiments, specifically designed to study the anisotropies of the CMB, have provided more precise limits to this parameter. We can mention the WMAP team results for the 1-year [18], 3-year [25] and 5-year [20] data releases, based on the angular bispectrum of the CMB. An independent analysis using the angular bispectrum was performed by [4, 5]. Some analyses on WMAP data used other methods as for example the Minkowski functionals [18, 25, 13, 15, 20], local curvature [2], etc. With respect to the balloon-borne experiments we can mention the recent analyses of the Archeops data using the Minkowski functionals [7, 8] and the analysis on the BOOMERanG data by [10]. In Table 1 we summarise the main results from the previous works.

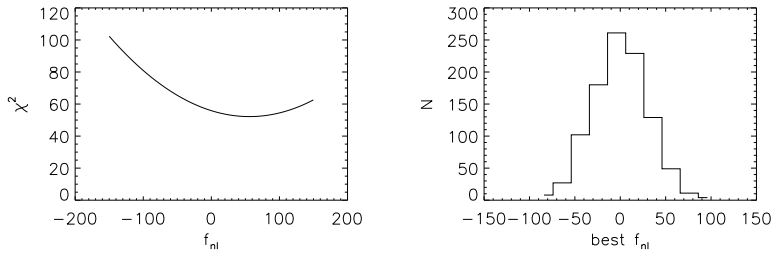

Fig. 2 From left to right, the $\chi^2(f_{nl})$ statistics for the WMAP combined V+W data map, and the histogram of the best fit f_{nl} values of a set of 1000 Gaussian simulations of the V+W map.

Table 1 Recent constraints on f_{nl} using different data sets and statistical tools.

Constraints (95% CL)	Method	CMB data	Reference
$-8 < f_{nl} < +111$	SMHW	WMAP-5	[9]
$-9 < f_{nl} < +111$	Angular bispectrum	WMAP-5	[20]
$-178 < f_{nl} < +64$	Minkowski functionals	WMAP-5	[20]
$-36 < f_{nl} < +100$	Angular bispectrum	WMAP-3	[5]
$+27 < f_{nl} < +147$	Angular bispectrum	WMAP-3	[26]
$-101 < f_{nl} < +107$	Genus[a]	WMAP-3	[13]
$-70 < f_{nl} < +91$	Minkowski Functionals	WMAP-3	[15]
$-54 < f_{nl} < +114$	Angular bispectrum	WMAP-3	[25]
$-180 < f_{nl} < +170$	Local Curvature & wavelets	WMAP-1	[2]
$-27 < f_{nl} < +121$	Angular bispectrum	WMAP-1	[4]
$-58 < f_{nl} < +134$	Angular bispectrum	WMAP-1	[18]
$-800 < f_{nl} < +1050$	Minkowski functionals	BOOMERanG	[10]
$-920 < f_{nl} < +1075$	Minkowski functionals	Archeops	[8]

[a] The Genus is one of the three Minkowski functionals on the sphere.

5 Conclusions

We have presented a review of the constraints on the f_{nl} parameter using the CMB. In particular, we have summarised the results obtained by [9] using wavelets, which provides the best constraints on the non-linear coupling parameter up to date, and compared it with other works. It is interesting to point out that this study includes, for the first time, inter-scale wavelet estimators to constrain the f_{nl} parameter. Their results are as good as those obtained by the WMAP team [20] using an optimal estimator based on the bispectrum (the so-called KSW) [19].

The WMAP data are compatible with Gaussianity and, in particular, the f_{nl} value that best fits the data is consistent with zero at the 95 per cent CL. This result is in agreement with most of the reported analyses, including the one of the WMAP team, and in disagreement with the non-zero f_{nl} reported by [9] (see [26] for a discussion of this result).

We emphasise the agreement found between the two estimators (the bispectrum [20] and the wavelets [9]), since they are formed by very different combinations of the data and therefore they are affected by systematic effects in very different ways.

Acknowledgements We acknowledge partial financial support from the Spanish Ministerio de Ciencia e Innovación project AYA2007-68058-C03-02. A. C. thanks the Spanish Ministerio de Ciencia e Innovación for a pre-doctoral fellowship. The authors acknowledge the computer resources, technical expertise and assistance provided by the Spanish Supercomputing Network (RES) node at Universidad de Cantabria.

References

1. Bartolo N., Komatsu E., Matarrese S., Riotto A., 2004, Phys. Rep., 402, 103
2. Cabella P., Liguori M., Hansen F. K., Marinucci D., Matarrese S., Moscardini L., Vittorio N., 2005, MNRAS, 358, 684
3. Cayón L., Martínez-González E., Argüeso F., Banday A. J., Górski K. M., 2003, MNRAS, 339, 1189
4. Creminelli P., Nicolis A., Senatore L., Tegmark M., & Zaldarriaga M. 2006, JCAP, 0605, 004
5. Creminelli P., Senatore L., Zaldarriaga M., & Tegmark M. 2007, JCAP, 0703, 005
6. Cruz M., Turok N., Vielva P., Martínez-González E., Hobson M., 2007, Science, 318, 1612
7. Curto A., Aumont J., Macías-Pérez J. F., Martínez-González E., Barreiro R. B., Santos D., Désert F. X., Tristram M., 2007, A&A, 474, 23
8. Curto A., Macías-Pérez J. F., Martínez-González E., Barreiro R. B., Santos D., Hansen F. K., Liguori M., Matarrese S., 2008, A&A, 486, 383
9. Curto A., Martínez-González E., Mukherjee P., Barreiro R. B., Hansen F. K., Liguori M., Matarrese S., 2008, submitted to MNRAS, arXiv:0807.0231
10. De Troia G., Ade P. A. R., Bock J. J., Bond J. R., Borrill J., Boscaleri A., Cabella P., Contaldi C. R., et al. 2007, ApJL, 670, L73
11. De Zotti G., Ricci R., Mesa D., Silva L., Mazzotta P., Toffolatti L., González-Nuevo J., 2005, A&A, 431, 893
12. Gangui A., Lucchin F., Matarrese S., Mollerach S., 1994, ApJ, 430, 447
13. Gott J. R., Colley W. N., Park C.-G., Park C., Mugnolo C., 2007, MNRAS, 377, 1668
14. Guth A. H., 1981, Phys. Rev. D, 23, 347
15. Hikage C., Matsubara T., Coles P., Liguori M., Hansen F. K., Matarrese S., 2008, MNRAS, 389, 1439
16. Komatsu E., Spergel D. N., 2001, Phys. Rev. D, 63, 063002
17. Komatsu E., Wandelt B. D., Spergel D. N., Banday A. J., & Górski K. M. 2002, ApJ, 566, 19
18. Komatsu E., Kogut A., Nolta M. R., Bennett C. L., Halpern M., Hinshaw G., Jarosik N., Limon M., Meyer S. S., Page L., Spergel D. N., Tucker G. S., Verde L., Wollack E., Wright E. L., 2003, ApJS, 148, 119
19. Komatsu E., Spergel D. N., & Wandelt B. D. 2005, ApJ, 634, 14
20. Komatsu E., Dunkley J., Nolta M. R., Bennett C. L., Gold B., Hinshaw G., Jarosik N., Larson D., Limon M., Page L., Spergel D. N., Halpern M., Hill R. S., Kogut A., Meyer S. S., Tucker G. S., Weiland J. L., Wollack E., Wright E. L., 2008, submitted to ApJS, ArXiv:0803.0547
21. Liguori M., Matarrese S., Moscardini L., 2003, ApJ, 597, 57
22. Liguori M., Yadav A., Hansen F. K., Komatsu E., Matarrese S., Wandelt B., 2007, Phys. Rev. D, 76, 105016
23. Martínez-González E., Gallegos J. E., Argüeso F., Cayón L., Sanz J. L., 2002, MNRAS, 336, 22
24. Salopek D. S., Bond J. R., 1990, Phys. Rev. D, 42, 3936
25. Spergel D. N., Bean R., Doré O., Nolta M. R., Bennett C. L., Dunkley J., Hinshaw G., Jarosik N., et al. 2007, ApJS, 170, 377
26. Yadav A. P. S., Wandelt B. D., 2008, Physical Review Letters,100, 181301